Journal of Energy Storage 55 (2022) 105474

Contents lists available at ScienceDirect

Journal of Energy Storage

journal homepage: www.elsevier.com/locate/est

Research papers

State of charge estimation of lithium-ion battery based on improved forgetting factor recursive least squares-extended Kalman filter joint algorithm

Caian Ge, Yanping Zheng *, Yang Yu

College of Automobile and Traffic Engineering, Nanjing Forestry University, Nanjing 210037, China

ARTICLE INFO

Keywords:
lithium-ion battery
On-line identification
Joint algorithm
SOC estimation

ABSTRACT

In order to solve the problem that forgetting factor recursive least squares (FFRLS) is prone to abnormal jitter and even divergence under complex working conditions, improved forgetting factor recursive least squares based on dynamic constraint and parameter backtracking is proposed. A joint algorithm of improved forgetting factor recursive least squares and extended Kalman filter (EKF) is used to estimate the state of charge (SOC) of lithium-ion battery. Firstly, parameters of Thevenin equivalent circuit model are identified on-line by the improved FFRLS considering dynamic constraint and parameter backtracking, and then the SOC of lithium-ion battery is estimated by extended Kalman filter. The results show that the improved forgetting factor recursive least squares has high accuracy of battery model parameters identification and the joint algorithm also has high accuracy and robustness of SOC estimation under dynamic stress test (DST) condition, the maximum absolute SOC estimation error is 2.49 % and the average absolute SOC estimation error is 1.39 %.

1. Introduction

With the growth of public demand, technological development and government support, new energy vehicles are becoming more and more popular. Lithium-ion power batteries have the advantages of large capacity and high energy, and are widely used in new energy vehicles [1]. Since the state of charge (SOC) estimation of lithium-ion power battery directly determines the control strategy of electric vehicle battery management system, and the accuracy of SOC estimation will affect the performance of electric vehicle, the battery SOC estimation is of great significance to the development of electric vehicle. At present, common SOC estimation methods mainly include ampere-hour integration method, open circuit voltage method, data-driven method, model-based method and Kalman filter method [2]. The initial SOC of ampere-hour integration method is difficult to obtain accurately, and the current measurement error will cause a more serious cumulative error after integration. Open circuit voltage method requires the battery to stand for a long time to obtain the open circuit voltage (OCV), which is not suitable for real-time SOC estimation [3,4]. Data-driven method has received widespread attention for its flexibility and model-free advantages [5]. This method can directly analyze the hidden information from the external characteristic parameters of the battery and has a high degree of non-linearity and self-learning characteristics. But the method depends on the accuracy of training data, and the method can't guarantee the accuracy of SOC estimation under complex and unknown working conditions [6,7]. Artificial neural network (ANN), fuzzy logic (Fuzzy Logic) and support vector machine (SVM) are commonly used data-driven methods. Electrochemical model mainly includes pseudo two dimensional model (P2D), single particle model (SP) and other simplified pseudo two dimensional model (SP2D). This model is accurate but its partial differential equations have no analytical solutions. Generally, the finite difference method is used to solve them, which takes a long time. Equivalent circuit model uses circuit components such as resistors, capacitors, and constant voltage sources to form a circuit network to simulate the dynamic characteristics of the battery. Kalman filter method based on battery equivalent circuit model has become a research hotspot for its low computational complexity, real-time and robustness [8,9]. The accuracy of battery equivalent circuit model directly affects the accuracy of SOC estimation when using Kalman filter method. In previous research, parameters of battery equivalent circuit model are usually obtained by off-line identification. For example, [10] used the hybrid pulse power characterization (HPPC) test to identify the

* Corresponding author.
E-mail address: zhengyp@njfu.com.cn (Y. Zheng).

https://doi.org/10.1016/j.est.2022.105474
Received 29 January 2022; Received in revised form 4 June 2022; Accepted 9 August 2022
Available online 8 September 2022

parameters of battery model off-line, and then used the extended Kalman filter (EKF) to estimate SOC. However, parameters of battery model identified off-line will not change with the battery service environment and cycle times. Therefore, some scholars proposed a method based on forgetting factor recursive least squares (FFRLS) to identify parameters of battery model on-line. For example, [11] established a second-order resistance capacitance equivalent circuit model of battery and used the unscented Kalman filter-extended Kalman filter (UKF-EKF) to update battery parameters and estimate SOC; [12] proposed an SOC estimation method based on lithium-ion battery equivalent circuit model, which overcome the state estimation problems of nonlinear and non-Gaussian error distribution caused by complex open circuit voltage characteristics by using sequential Monte Carlo filter; [13] used forgetting factor recursive least squares to identify parameters of lithium-ion super capacitor model. On the basis of obtaining accurate super capacitor model parameters, adaptive square root-untraced Kalman filter (ASR-UKF) was used to realize the accurate estimation of super capacitor SOC; [14] introduced a novel splice Kalman filtering algorithm with adaptive robust performance to improve the charged state prediction accuracy of the lithium ion battery pack. However, forgetting factor recursive least squares is easy to cause large fluctuation and even negative value in identification of battery model parameters. Therefore, this paper selects ternary lithium battery as research object, proposes a joint algorithm of improved FFRLS-EKF to estimate battery SOC based on Thevenin equivalent circuit model, and verifies the accuracy and robustness of the battery SOC estimation under dynamic stress test (DST) condition.

2. Establishment of ternary lithium battery model

2.1. Equivalent circuit model

Equivalent circuit model characterizes characteristics of battery through a specific circuit. The accuracy of equivalent circuit model directly affects the accuracy of battery SOC estimation. [15] studied several equivalent circuit models, the results show that the accuracy of equivalent circuit model is not always improved by increasing the number of RC rings; on the contrary, over fitting problem occurs with a certain probability. [16] proved that Thevenin equivalent circuit model is more suitable for ternary lithium battery compared with other twelve equivalent circuit models. Moreover, compared with Rint model, Thevenin model can better reflect the dynamic characteristics of lithium-ion battery; compared with PNGV (Partnership for a New Generation of Vehicles) model and GNL (General Nonlinear) model, Thevenin model has moderate complexity and the parameter identification of Thevenin model is easier. Therefore, considering characteristics of research object, accuracy of battery model and complexity of SOC estimation algorithm, this paper selects Thevenin equivalent circuit model which is shown in Fig. 1.

In Fig. 1: U_{oc} is the open circuit voltage, U_t is the terminal voltage, I is the operating current, which is taken as positive when discharging, R_0 is the ohmic internal resistance, R_1 is the polarization internal resistance, C_1 is the polarization capacitance, U_1 is the polarization voltage. According to the electrical engineering theory, the electrical relationship of Thevenin equivalent circuit model can be obtained as:

$$\begin{cases} U_{oc}(t) = I(t)R_0(t) + U_1(t) + U_t(t) \\ I(t) = C_1(t)\dfrac{dU_1(t)}{dt} + \dfrac{U_1(t)}{R_1(t)} \end{cases} \tag{1}$$

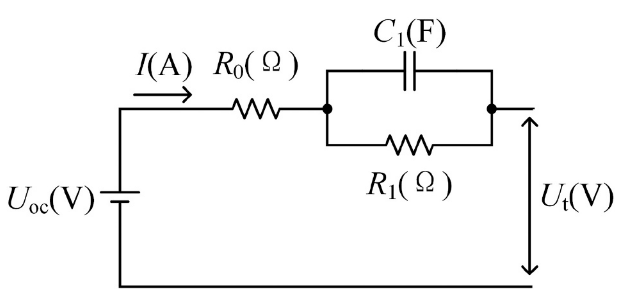

Fig. 1. Thevenin equivalent circuit model.

2.2. Open circuit voltage model

In this paper, the SOC-OCV curve of ternary lithium battery is fitted by polynomial through HPPC test. Polynomial fitting curves of different orders are shown in Fig. 2. It can be seen from Fig. 2 that the polynomial fitting curves of three different orders can fit the real open circuit voltage well when SOC is 0.15–0.9, but the fitting results are different when SOC is 0.05–0.1 or 0.95–1. When the polynomial order is 9, there is over fitting compared with 6-order polynomial. When the polynomial order is 4, the fitting accuracy is lower compared with 6-order polynomial. Therefore, in this paper, 6-order polynomial is selected to fit the SOC-OCV curve, and the fitting formula is:

$$\begin{aligned} U_{oc} &= -43.56SOC^6 + 155.4SOC^5 - 215.7SOC^4 \\ &+146.6SOC^3 - 50.16SOC^2 + 8.674SOC + 3.12 \end{aligned} \tag{2}$$

3. Joint SOC estimation of ternary lithium battery

3.1. Forgetting factor recursive least squares

When using forgetting factor recursive least squares to identify parameters of Thevenin model, Thevenin model needs to be transformed into the basic form of least squares (LS). According to the electrical engineering theory, the electrical relationship of Thevenin model is expressed in s domain:

$$\frac{U_t(s) - U_{oc}(s)}{I(s)} = R_0 + \frac{R_1}{\tau s + 1} \tag{3}$$

In Eq. (3), s is the Laplacian in s domain, $\tau = R_1C_1$.

Continuous time system can be transformed into discrete time system by bilinear transformation [17]:

$$s = \frac{2}{T_s}\frac{1 - z^{-1}}{1 + z^{-1}} \tag{4}$$

In Eq. (4), T_s is the sampling period, which value is 1 s in this paper.

Discrete Eq. (3) with Eq. (4):

$$\frac{U_{t,k} - U_{oc,k}}{I_k} = \frac{\theta_{2,k} + \theta_{3,k}z^{-1}}{1 + \theta_{1,k}z^{-1}} \tag{5}$$

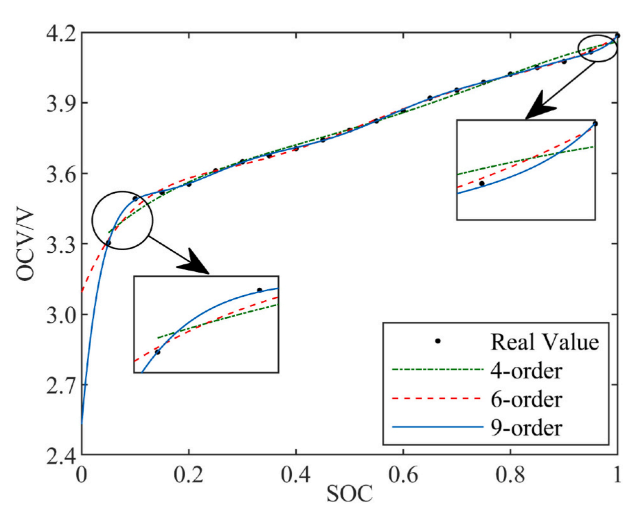

Fig. 2. SOC-OCV fitting curve under different orders.

In Eq. (5), subscript k represents discrete time k, $\theta_{1,k}$, $\theta_{2,k}$, $\theta_{3,k}$ are the parameters to be estimated at discrete time k, and the calculation expression is as follows:

$$\begin{cases} \theta_{1,k} = -\dfrac{T_s - 2\tau_k}{T_s + 2\tau_k} \\ \theta_{2,k} = -\dfrac{R_{0,k}T_s + R_{1,k}T_s + 2R_{0,k}\tau_k}{T_s + 2\tau_k} \\ \theta_{3,k} = -\dfrac{R_{0,k}T_s + R_{1,k}T_s - 2R_{0,k}\tau_k}{T_s + 2\tau_k} \end{cases} \tag{6}$$

Because U_{oc} can only be obtained after the battery has stood for a long time, it can't be measured real-time, and large error will be introduced in the process of obtaining U_{oc}. Therefore, in this paper, U_{oc} is taken as a parameter to be identified, and Eq. (5) can be changed to:

$$U_{t,k} = \theta_{1,k}U_{t,k-1} + \theta_{2,k}I_k + \theta_{3,k}I_{k-1} + \theta_{4,k} \tag{7}$$

In Eq. (7), $\theta_{4,k} = U_{oc,k} - U_{oc,k-1}\theta_{1,k}$.

After identifying $\theta(k)$, the parameters of Thevenin model can be obtained as follows:

$$\begin{cases} U_{oc,k} = \theta_{1,k} + U_{oc,k-1}\theta_{2,k} \\ R_{0,k} = \dfrac{\theta_{4,k} - \theta_{3,k}}{1 + \theta_{2,k}} \\ R_{1,k} = \dfrac{\theta_{3,k} + \theta_{4,k}}{\theta_{2,k-1}} - R_{0,k} \\ \tau_k = \dfrac{T_s\left(1 + \theta_{2,k}\right)}{2\left(1 - \theta_{2,k}\right)} \end{cases} \tag{8}$$

Transform Thevenin model into the basic form of least squares:

$$\hat{y}_k = \phi_k^T \theta_k = \hat{U}_{t,k} \tag{9}$$

In Eq. (9), φ_k is the input vector, θ_k is the estimated parameter vector, and the calculation expression is as follows:

$$\begin{cases} \phi_k = \left[1, U_{t,k-1}, I_k, I_{k-1}\right]^T \\ \theta_k = \left[\theta_{4,k}, \theta_{1,k}, \theta_{2,k}, \theta_{3,k}\right]^T \end{cases} \tag{10}$$

Set the gain coefficient as K_k, the estimated parameter as θ_k, the covariance matrix as P_k, and the forgetting factor as λ. Equation of the forgetting factor recursive least squares is:

$$\begin{cases} K_k = P_{k-1}\phi_k^T\left[\phi_k P_{k-1}\phi_k^T + \lambda\right]^{-1} \\ \theta_k = \theta_{k-1} + K_k\left[\hat{y}_k - \phi_k^T\theta_{k-1}\right] \\ P_k = \left[I - K_k\phi_k^T\right]P_{k-1}\lambda^{-1} \end{cases} \tag{11}$$

The forgetting factor recursive least squares adjusts the weight of new and old data by forgetting factor λ ($0 < \lambda < 1$) which is generally between 0.95 and 0.99 [18]. The smaller λ, the greater the weight of new data and the better the system tracking effect, but the greater the fluctuation of parameter identification result. The larger λ, the greater the weight of old data and the worse the system tracking effect, but the smaller the fluctuation of parameter identification result.

3.2. Improved forgetting factor recursive least squares

When using forgetting factor recursive least squares to identify battery model parameters, it is expected that the terminal voltage error is small, so take $\lambda = 0.95$. The identification result of polarization internal resistance R_1 of a certain type of ternary lithium battery is shown in Fig. 3. As can be seen from Fig. 3, except that the identification result is negative due to improper initial value setting of the algorithm, the identification result still has negative value and abnormal jitter during the whole identification process. Then take $\lambda = 0.99$, the identification result of polarization internal resistance R_1 is shown in Fig. 4. As can be

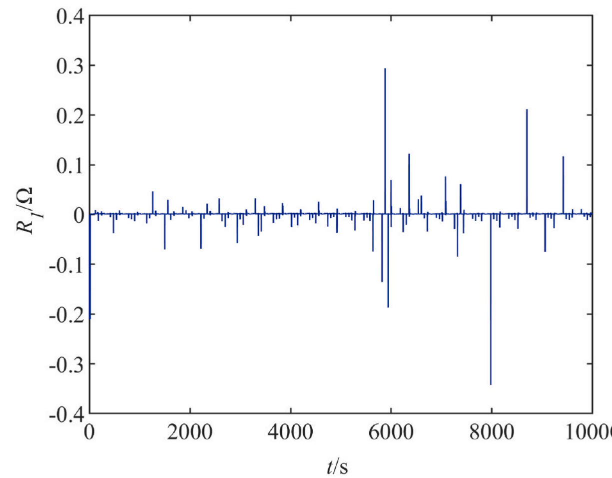

Fig. 3. Polarization internal resistance identification result ($\lambda = 0.95$).

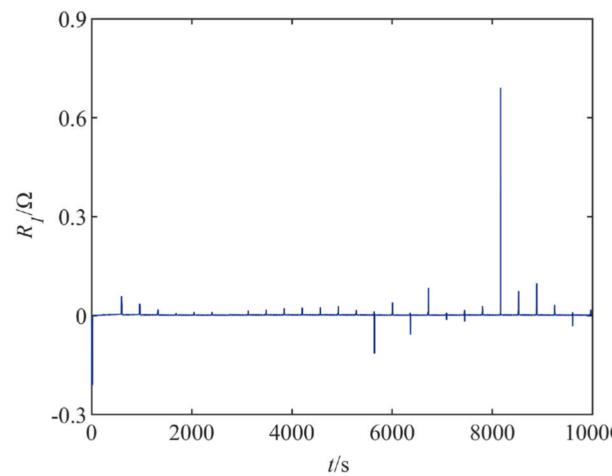

Fig. 4. Polarization internal resistance identification result ($\lambda = 0.99$).

seen from Fig. 4, the identification result is better, but still has fewer negative value and abnormal jitter.

Forgetting factor recursive least squares is prone to abnormal jitter and even divergence, so it is necessary to improve forgetting factor recursive least squares [19]. Firstly, this paper calculates the mean μ and standard deviation σ of the identification result at first 100 times, and dynamically sets upper boundary of the identification result as $\mu + 3\sigma$ and lower boundary as the larger value of 0 and $\mu - 3\sigma$. If the identification result at discrete time k is not within the boundary value, the identification result will be changed to the corresponding boundary value. Then calculate the terminal voltage error with dynamically constrained battery model parameters. If the terminal voltage error is <0.05 V, output the identification result; otherwise, perform 40 steps parameter backtracking, and output the identification result that minimizes the terminal voltage error in 40 steps parameter backtracking. Fig. 5 shows the comparison result of polarization internal resistance of two algorithms. It can be seen from Fig. 5 that the identification result of the improved forgetting factor recursive least squares is better. The flow chart of improved forgetting factor recursive least squares is shown in Fig. 6.

3.3. Extended Kalman filter

The expression for calculating battery SOC by ampere-hour integral method is:

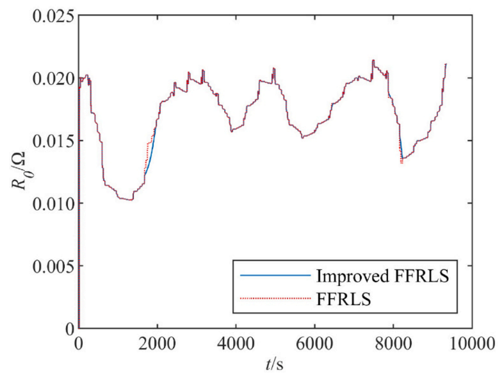

(a) the ohmic internal resistance

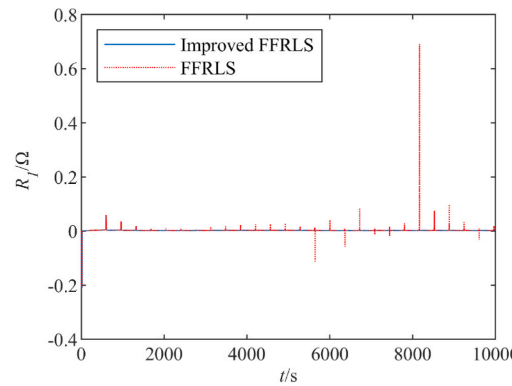

(b) the polarization internal resistance

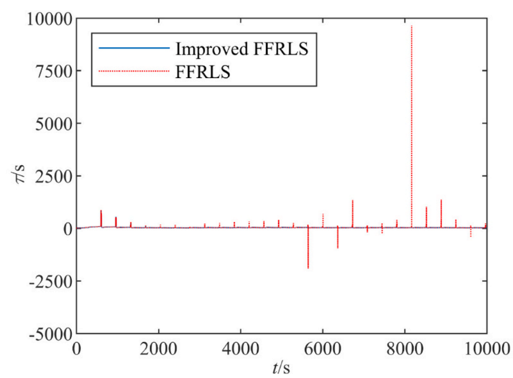

(c) the time constant

Fig. 5. Comparison result of polarization internal resistance identification ($\lambda = 0.99$).

$$SOC(t) = SOC_0 - \int_0^t I(t)\mathrm{d}t \Big/ C_\mathrm{N} \tag{12}$$

In Eq. (12), SOC_0 is the initial value of SOC, C_N is the capacity of the battery.

According to Eqs. (1) and (12), the discrete state-space equation of battery can be obtained with $[U_1, SOC]^\mathrm{T}$ as the system state variable x, U_t as the system output variable y, I as the system input variable u, w (the mean of w is 0 and the covariance is Q) as the state noise and v (the mean of v is 0 and the covariance is R) as the observation noise:

$$\begin{cases} x_{k+1} = f(x_k, u_k) + w_k \\ y_k = g(x_k, u_k) + v_k \end{cases} \tag{13}$$

Because f and g functions in the battery model are nonlinear, it is impossible to use Kalman filter (KF) directly to estimate SOC. Therefore, extended Kalman filter is used to estimate SOC in this paper. Its basic idea is to linearize the nonlinear function by first-order Taylor series [20]. The state-space equation of battery is:

$$\begin{cases} x_{k+1} = A_k x_k + B_k u_k + w_k \\ y_k = C_k x_k + D_k u_k + v_k \end{cases} \tag{14}$$

The SOC estimation process based on extended Kalman filter is as follows [21]:

1. Linearize the nonlinear functions by first-order Taylor series:

$$\begin{cases} A_k = \begin{bmatrix} e^{-T_\mathrm{s}/\tau} & 0 \\ 0 & 1 \end{bmatrix} \\ B_k = \begin{bmatrix} R_1\left(1 - e^{-T_\mathrm{s}/\tau}\right) \\ -T_\mathrm{s}/C_\mathrm{N} \end{bmatrix} \\ C_k = \begin{bmatrix} -1 & \dfrac{\partial U_\mathrm{oc}}{\partial SOC_k}\Big|_{x_k = \widehat{x}_k} \end{bmatrix} \\ D_k = [-R_0] \end{cases} \tag{15}$$

2. Initialize system state variable $\widehat{x}$ and covariance P:

$$\begin{cases} \widehat{x}_0 = E[x] \\ \widehat{P}_0 = E\left[(x - \widehat{x}_0)(x - \widehat{x}_0)^\mathrm{T}\right] \end{cases} \tag{16}$$

3. One-step prediction of system state variable $\widehat{x}$ and covariance P:

$$\begin{cases} \widehat{x}_k^- = f\left(\widehat{x}_{k-1}^+, u_{k-1}\right) \\ \widehat{P}_k^- = A_{k-1}\widehat{P}_{k-1}^+ A_{k-1}^T + Q_{k-1} \end{cases} \tag{17}$$

4. Update Kalman filter gain K_k:

$$K_k = \widehat{P}_k^- C_k^T \left(C_k \widehat{P}_k^- C_k^T + R_k\right)^{-1} \tag{18}$$

5. Update system state variable $\widehat{x}$ and covariance P:

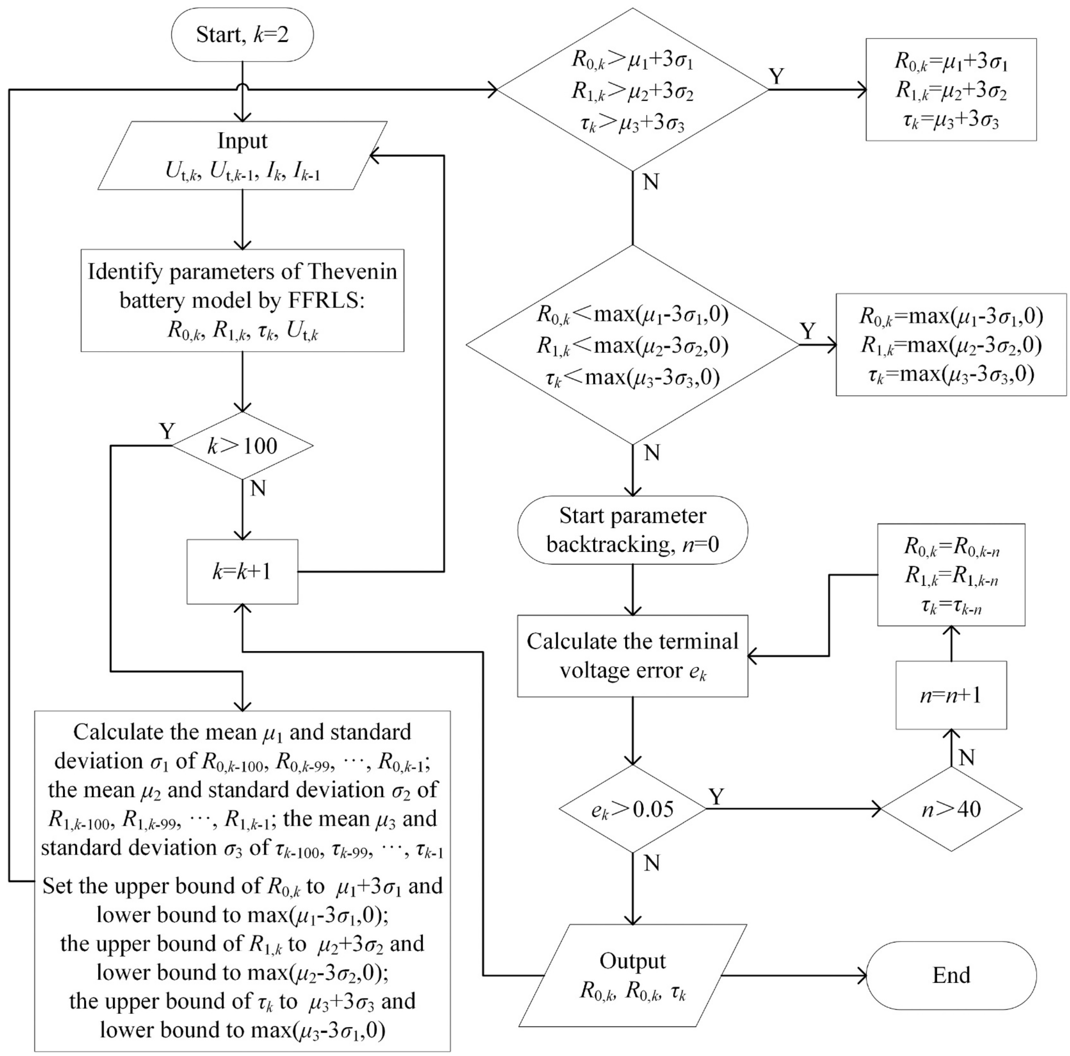

Fig. 6. Flow chart of improved FFRLS.

$$\begin{cases} \hat{x}_k^+ = \hat{x}_k^- + K_k\left(U_{t,k} - C_k\hat{x}_k^-\right) \\ \hat{P}_k^+ = (I - K_kC_k)\hat{P}_k^- \end{cases} \tag{19}$$

3.4. Improved FFRLS combined with EKF to estimate SOC

Battery model parameters R_0, R_1, τ, U_{oc} are identified by improved forgetting factor recursive least squares on-line, then the parameters are used to estimate SOC by extended Kalman filter, and according to the SOC-OCV curve, U_{oc} at discrete time k is obtained for battery model parameter identification at discrete time $k+1$.

4. Test and simulation analysis

4.1. Battery test platform

This paper selects ternary lithium power battery produced by LG Company as the research object. Table 1 lists rated parameters of the power battery. Battery test platform is shown in Fig. 7. The maximum charge and discharge voltage of the BT-2016E battery tester is 5 V (voltage accuracy: 0.005 V), and the maximum charge and discharge current is 200A (current accuracy: 0.02A). It is connected to the positive and negative poles of the battery through the power cord. SPX-150BE incubator has a temperature control range of 0–70 °C and a temperature control accuracy of 0.1 °C. The internal temperature can be adjusted through the control panel. The computer is the control center and data recording center of the battery test platform. It is responsible for controlling the charging and discharging methods of the battery tester, charging and discharging current, and recording voltage of the battery. All tests in this paper are carried out at 25 °C.

Table 1
Rated parameters of LG ternary lithium power battery.

Parameter	Value
Size (mm)	232 × 160.3 × 7.51
Capacity (Ah)	27
Nominal voltage (V)	3.7
Charge cut-off voltage (V)	4.3
Discharge cut-off voltage (V)	2.75
Mass (g)	560
Charging temperatures (°C)	0–45
Discharging temperatures (°C)	−20–60
Storage temperatures (°C)	−20–35

4.2. Accuracy verification of equivalent circuit model

Refer to the electric vehicle battery test manual to perform dynamic stress test on the battery. Dynamic stress test is a series of constant power discharge/charge steps with a total duration of 360 s, the current of a dynamic stress test cycle is shown in Fig. 8. Dynamic stress test cycles are

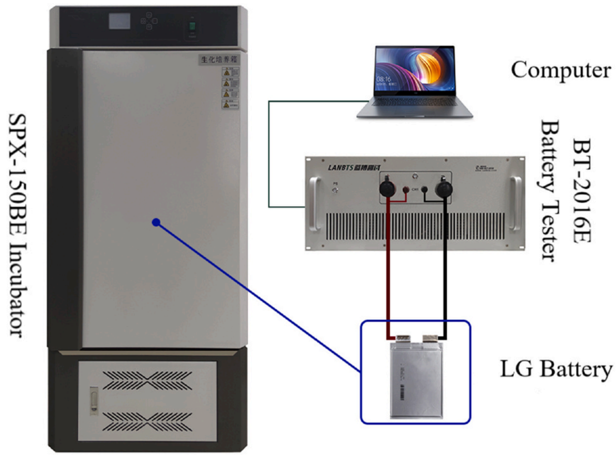

Fig. 7. Battery test platform.

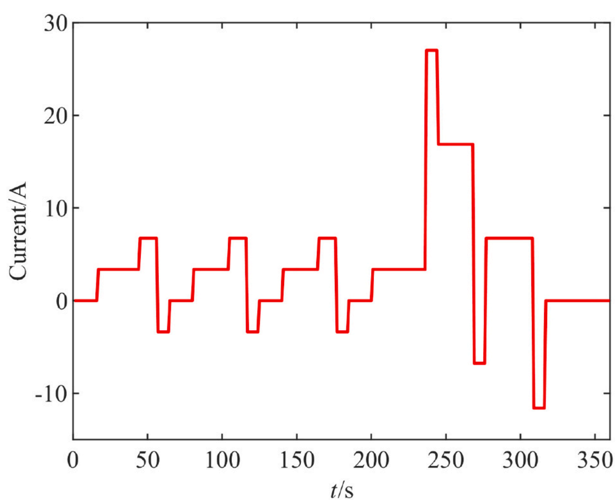

Fig. 8. Current of a dynamic stress test cycle.

set to discharge the battery capacity from 100 % to about 10 %. The terminal voltage comparison is shown in Fig. 8. Since the current flowing through the battery is measured by the high-accuracy BT-2016E battery tester, SOC calculated by ampere-hour integration method can be seen as the real value of the SOC. It can be seen from Fig. 9 that the terminal voltage of each algorithm can follow real terminal voltage well. The average absolute terminal voltage error of forgetting factor recursive least squares is 3.02 mV, and the average absolute terminal voltage error of improved forgetting factor recursive least squares is 0.37 mV, which shows that the accuracy of the battery model parameters identified by improved forgetting factor recursive least squares is higher than that of forgetting factor recursive least squares under dynamic stress test condition.

4.3. Battery SOC estimation verification

Forgetting factor recursive least squares and improved forgetting factor recursive least squares are combined with extended Kalman filter to estimate SOC of ternary lithium battery. The real SOC is calculated by ampere-hour integral method, and the initial SOC of the battery is 1. The estimation result is shown in Fig. 10 and the absolute SOC estimation error is shown in Fig. 11. It can be found from Fig. 10 that when SOC > 0.9, SOC estimation error is small, and SOC estimation error increases with the decrease of SOC. As can be seen from Fig. 11, the maximum absolute SOC estimation error of FFRLS-EKF joint algorithm is 2.62 %, and the average absolute SOC estimation error of FFRLS-EKF joint algorithm is 1.54 %; the maximum absolute SOC estimation error of the improved FFRLS-EKF joint algorithm is 2.49 %, and the average absolute SOC estimation error of the improved FFRLS-EKF joint algorithm is 1.39 %. Compared with the FFRLS-EKF joint algorithm, the SOC estimation accuracy of the improved FFRLS-EKF joint algorithm is improved by 9.74 %.

The initial SOC of the battery is difficult to obtain. In order to verify the robustness of the improved FFRLS-EKF joint algorithm proposed in this paper, the initial values of SOC are set to error values of 0.9, 0.7 and 0.5. The SOC estimation result under different SOC initial errors is shown in Fig. 12. As can be seen from Fig. 12, under different SOC initial errors, the SOC estimation result can converge to the real SOC in a short time, and the time required for convergence increases with the increase of SOC initial error. In conclusion, the improved FFRLS-EKF joint algorithm has good robustness.

5. Conclusions

In order to improve the accuracy of on-line identification of battery model parameters and eliminate large fluctuation or even negative value of on-line identification of battery model parameters by forgetting factor recursive least squares, based on Thevenin equivalent circuit model, this paper uses the improved forgetting factor recursive least squares to identify the battery model parameters on-line, and then uses extended

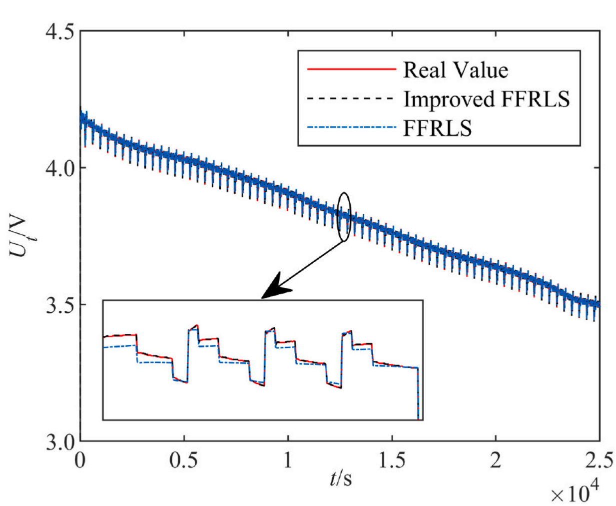

Fig. 9. Terminal voltage comparison.

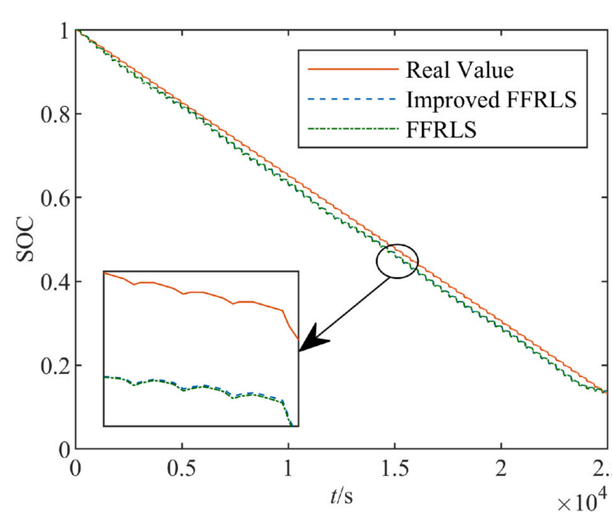

Fig. 10. SOC estimation result.

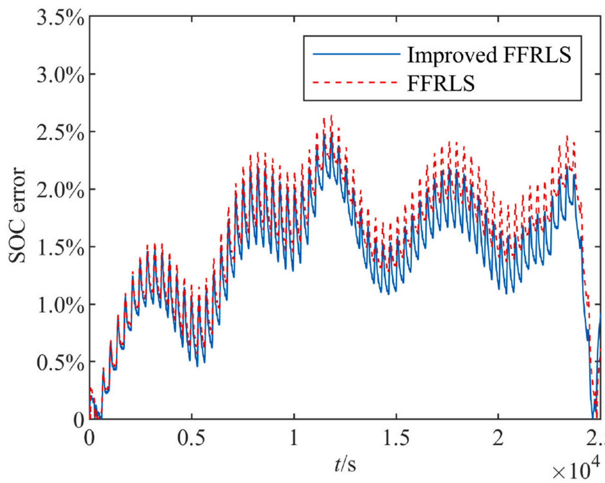

Fig. 11. SOC estimation error comparison.

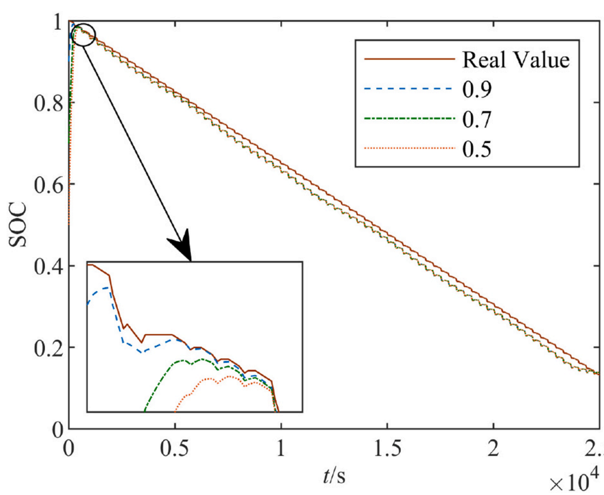

Fig. 12. SOC estimation result under different SOC initial errors.

Kalman filter to estimate battery SOC based on the dynamically updated battery model parameters. The test and simulation results show that the maximum absolute SOC estimation error is 2.49 % and the average absolute SOC estimation error is 1.39 % under dynamic stress test condition. When the SOC initial error is large, the battery SOC can still converge to the real SOC in a short time.

CRediT authorship contribution statement

Caian Ge: Conceptualization, Methodology, Writing - original draft, Writing - review & editing. **Yanping Zheng**: Supervision, Funding acquisition, Investigation. **Yang Yu**: Software, Project administration.

Declaration of competing interest

The authors declare that they have no known competing financial interests or personal relationships that could have appeared to influence the work reported in this paper.

Data availability

The authors do not have permission to share data.

Acknowledgements

This work is financially supported by National Natural Science Foundation of China (51975299), Jiangsu Provincial Key Research and Development Program (BE2017008).

References

[1] X. Lin, Y. Tang, J. Ren, Y. Wei, State of charge estimation with the adaptive unscented Kalman filter based on an accurate equivalent circuit model, J. Energy Storage 41 (2021), 102840.
[2] D. Andre, C. Appel, T. Soczka-Guth, D.U. Sauer, Advanced mathematical methods of SOC and SOH estimation for lithium-ion batteries, J. Power Sources 224 (2013) 20–27.
[3] J.W. Shen, J. Xiong, X. Shu, G. Li, Y.J. Zhang, Z. Chen, Y.G. Liu, State of charge estimation framework for lithium-ion batteries based on square root cubature Kalman filter under wide operation temperature range, Int. J. Energy Res. 45 (2020) 5586–5601.
[4] R. Xiong, H.W. He, F.C. Sun, K. Zhao, Evaluation on state of charge estimation of batteries with adaptive extended Kalman filter by experiment approach, IEEE Trans. Veh. Technol. 62 (2013) 108–117.
[5] S.L. Wang, C. Fernandez, C.M. Yu, Y.C. Fan, W. Cao, D. Store, A novel charged state prediction method of the lithium ion battery packs based on the composite equivalent modeling and improved splice Kalman filtering algorithm, J. Power Sources 471 (2020), 228450.
[6] M. Ye, H. Guo, B.B. Cao, A model-based adaptive state of charge estimator for a lithium-ion battery using an improved adaptive particle filter, Appl. Energy 190 (2017) 740–748.
[7] Q. Wang, H.R. Gu, M. Ye, M. Wei, X.X. Xu, State of charge estimation for lithium-ion battery based on NARX recurrent neural network and moving window method, IEEE Access 9 (2021) 83364–83375.
[8] C. Chen, R. Xiong, R.X. Yang, W.X. Shen, F.C. Sun, State-of-charge estimation of lithium-ion battery using an improved neural network model and extended Kalman filter, J. Clean. Prod. 234 (2019) 1153–1164.
[9] H.S. Ramadan, M. Becherif, F. Claude, Extended Kalman filter for accurate state of charge estimation of lithium-based batteries: a comparative analysis, Int. J. Hydrog. Energy 42 (2017) 29033–29046.
[10] Y.D. Xu, M.H. Hu, A.J. Zhou, Y.X. Li, S.X. Li, C.Y. Fu, C.C. Gong, State of charge estimation for lithium-ion batteries based on adaptive dual Kalman filter, Appl. Math. Model. 77 (2020) 1255–1272.
[11] G.T. Cui, W.H. Jiang, W. Tu, SOC estimation of lithium battery based on extended Kalman filter algorithm, Appl.Electron.Tech. 47 (2021) 36–39.
[12] Y.L. Zheng, F. He, W.L. Wang, A method to identify lithium battery parameters and estimate SOC based on different temperatures and driving conditions, Electronics 8 (2019) 1391–1405.
[13] G.Z. Dong, Z.H. Chen, J.W. Wei, Sequential Monte Carlo filter for state-of-charge estimation of lithium-ion batteries based on auto regressive exogenous model, IEEE Trans. Ind. Electron. 66 (2019) 8533–8544.
[14] S.L. Wang, S.Y. Jin, D.K. Bai, Y.C. Fan, H.T. Shi, C. Fernandez, A critical review of improved deep learning methods for the remaining useful life prediction of lithium-ion batteries, Energy Rep. 7 (2021) 5562–5574.
[15] T. Lv, X.X. Zhang, State of charge co-estimation of lithium-ion capacitor based on online parameter identification and ASR-UKF, Chin.J. Power Sources 45 (2021) 27–30+55.
[16] X. Lai, Y.J. Zheng, T. Sun, A comparative study of different equivalent circuit models for estimating state-of-charge of lithium-ion batteries, Electrochim. Acta 259 (2018) 566–577.
[17] X.S. Hu, S.B. Li, H. Peng, A comparative study of equivalent circuit models for Li-ion batteries, J. Power Sources 198 (2012) 359–367.
[18] P. Lin, X.M. Xu, X.L. Wu, H.P. Lee, Establishment and experimental verification of the sound absorption model of jute fiber felts, in: Noise and vibration Control 41, 2021, pp. 232–236+266.
[19] Z.H. Pang, H. Cui, in: System Identification and Adaptive Control MATLAB Simulation, 1st ed., Beijing University of Aeronautics and Astronautics Press, Beijing, China, 2013, pp. 30–45.
[20] H. Wang, Y.P. Zheng, Y. Yu, Lithium iron phosphate battery SOC estimation based on the least squares online identification of dynamic optimal forgetting factor, Automob.Technol. 38 (2021) 23–29.
[21] X.M. Xu, L. Zhang, K. Liu, N. Chen, Research on active steering control of trailer wheels for a tractor-semitrailer, Automob.Technol. 35 (2018) 36–40.